DOI: 10.1002/chem.200800545

Mechanisms of Air Oxidation of Ethoxylated Surfactants—Computational Estimations of Energies and Reaction Behaviors

Carina Bäcktorp,* Anna Börje, J. Lars G. Nilsson, Ann-Therese Karlberg, Per-Ola Norrby, and Gunnar Nyman[a]

Abstract: Pathways for formation of previously observed autoxidation products of ethoxylated surfactants have been studied by DFT (B3LYP). In addition to the established radical-chain reaction, several mechanistic possibilities for intramolecular fragmentation of the intermediate radicals have been characterized concerning reaction barriers and energies of transition states. The results can rationalize the formation of previously observed autoxidation products, including several, which have been implicated as strongly allergenic.

Keywords: allergens · autoxidation · density functional calculations · ethoxylated surfactants · radicals

Introduction

It is important to be able to assess the risks of skin allergies by means of predictive tests. The present work is part of our ongoing investigations of chemicals that can form allergenic oxidation products on air exposure, for example, at handling and storage. Many of these chemicals are not allergenic themselves or have only a low allergenic activity. This is the case for ethoxylated surfactants that are widely used in household and industrial cleaners, in topical pharmaceuticals, cosmetics, and laundry products. Combining experimental and computational efforts will provide more knowledge and insight about autoxidation of organic compounds. In this way, the understanding of structure-activity relationships (SAR) involving oxidative activation steps is increased and the basis for prediction of skin sensitizers (contact allergens) based on chemical structure is enlarged.

The ethoxylated surfactants are polyethers and as such oxidized by atmospheric oxygen, a fact that has been discussed in the surfactant literature.[1,2] In previous experimental studies,[3] we have shown that autoxidation of nonionic alcohol ethoxylates generates products that are skin sensitizers. Specific oxidation products, like hydroperoxides, formaldehyde, ethoxylated aldehydes, and ethoxylated formates, have been identified in autoxidation mixtures of the pure ethoxylated alcohol pentaethylene glycol mono-*n*-dodecyl ether ($C_{12}E_5$; Scheme 1a) used as reference surfactant.[3] Two hydroperoxides were identified, namely, 1-hydroperoxy-3,6,9,12,15-pentaoxaheptacosan-1-ol (Scheme 1c) and 16-hydroperoxy-3,6,9,12,15-pentaoxaheptacosan-1-ol (Scheme 1d), the latter being the dominating hydroperoxide in the oxidation mixture.[8] The major oxidation product

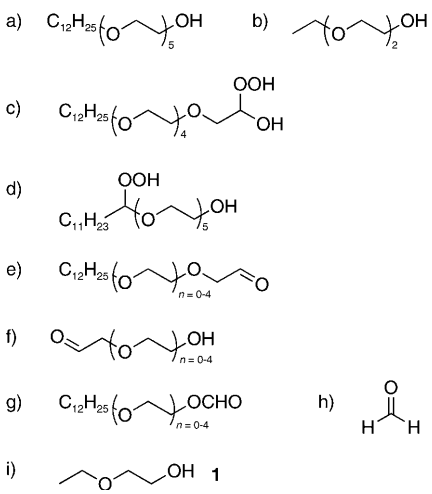

Scheme 1. The ethoxylated alcohols pentaethylene glycol mono-*n*-dodecyl ether ($C_{12}E_5$, a) and diethyleneglycol monoethylether (C_2E_2, b), major autoxidation products of $C_{12}E_5$ previously identified and investigated in experimental studies (c–h), and the theoretical model surfactant used in the present study (**1**).

[a] Dr. C. Bäcktorp, Dr. A. Börje, Prof. Dr. J. L. G. Nilsson, Prof. Dr. A.-T. Karlberg, Prof. Dr. P.-O. Norrby, Prof. Dr. G. Nyman
Department of Chemistry, University of Gothenburg
412 96 Gothenburg (Sweden)
Fax: (+46) 31-772-3840
E-mail: carina@chem.gu.se

Supporting information for this article is available on the WWW under http://dx.doi.org/10.1002/chem.200800545.

found was dodecyltetraoxyethyleneoxy acetaldehyde (Scheme 1e, $n=4$).[4] Autoxidized $C_{12}E_5$ was demonstrated to be allergenic in sensitization studies[3] and proved to have a significantly higher skin-irritating potential than the pure surfactant.[5] Of the products identified on autoxidation, all but ethoxylated formates (Scheme 1g) were shown to be contact allergens.[4,6,7,8,9] The corresponding results, formation of aldehydes, hydroperoxides, and formates during autoxidation, were also obtained when a model ethoxylated surfactant, diethyleneglycol monoethylether (C_2E_2; Scheme 1b), was exposed to air.[10]

Formation of hydroperoxides by autoxidation is described to proceed by a radical-chain reaction (Scheme 2).[1] Step I is the initiation step, in which a radical abstracts a hydrogen

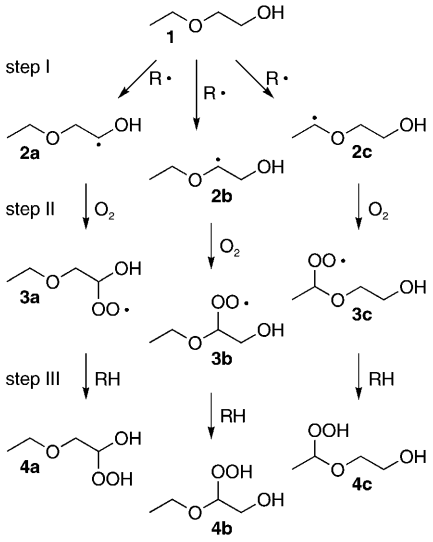

Scheme 2. The traditional intermolecular radical-chain reaction mechanism for autoxidation[1] illustrated for model compound **1**.

atom from the substrate. The propagation continues in two steps, step II, addition of oxygen, and step III, hydrogen abstraction from an adjacent molecule along with generation of a new radical that can continue the radical-chain reaction (step III for one molecule of substrate can thus be step I for another molecule). The chain mechanism is terminated when two radicals react to give stable molecules, a rare occurrence unless the radicals are unusually stable.[1] In the current study, we will only consider the products from the propagation steps, not the insignificant amounts produced by radical-chain termination.

The exothermic addition of oxygen to the radical in step II occurs without any reaction barrier;[11] hence, the rate-determining step of the propagation is when a hydrogen atom is abstracted, that is, step I or III (Scheme 2). The ease of formation of each type of radical (**2a**, **2b**, or **2c**), therefore, determines the initially selected autoxidation path. From earlier work,[11] we expect step II to be exergonic, whereas step III may well be endergonic. The initially formed distribution of hydroperoxide products will thus be determined both by step I and by the competition of step III with alternative degradation paths.

The hydroperoxide products **4** can give rise to secondary oxidation products through well-established rearrangements and fragmentations. For example, **4a** (a perhydrate) would be expected to be in rapid equilibrium with free aldehyde and hydrogen peroxide in the slightly acidic autoxidation mixture. However, there is also some precedent in the literature for direct fragmentation of radicals **3** to various carbonyl compounds[1] with simultaneous liberation of hydroperoxyl or hydroxyl radicals, which are also competent agents for propagation of the radical-chain reaction.

The aim of the present study was to use computational methods to elucidate reaction barriers and energies of transition states and intermediary free radicals in the autoxidation of the model compound ethyleneglycol monoethyl ether (**1**; Scheme 2), in order to elucidate the mechanism for formation of the observed oxidation. In the long term, the current study forms a part of a larger project to predict the potential formation of allergenic products produced upon air exposure of otherwise innocuous compounds.

Methods

We have employed DFT with the hybrid functional B3LYP[12] and the 6-31+G(d,p) basis set to optimize geometries and characterize stationary points in the potential-energy surface as minima or saddle points. Unrestricted methods were used for all open-shell species (radicals and the triplet biradical O_2). Harmonic vibrational frequencies have been used to calculate the thermodynamic contributions to the enthalpies and free energies. We have also verified the connectivity between a given transition state (TS) with the corresponding reactant and product by following the intrinsic reaction coordinate (IRC). The calculations were carried out by using the Gaussian 03 program package,[13] with molecule **1** as a model for the more complex ethoxylated alcohols shown in Scheme 1.

Results and Discussion

We will first consider the radical-chain pathways depicted in Scheme 2. The reaction energies (enthalpies and free energies) are shown in Table 1. The combination of free radical with O_2, step II, is barrierless,[11] strongly exothermic, and, even though the molecularity decreases, also strongly exergonic. This is in contrast to our earlier studies of unsaturated terpenes, in which the high stability of allylic radicals led to an almost isoergic combination with O_2.[11] The hydroperoxyl radicals **3** can, in principle, dissociate back to the reactants (**2**+O_2), but in the current case, such a reversion is very unfavorable and should not have any influence on the outcome of the reaction.

For the intermolecular hydrogen abstraction, steps I and III, we used **3a** as a model radical to test the relative re-

Table 1. Calculated reaction energies for the radical chain mechanism.

	ΔH°_0 [kcal mol^{-1}]	ΔH°_{298} [kcal mol^{-1}]	ΔG°_{298} [kcal mol^{-1}]
R$^\bullet$+O$_2$→ROO$^\bullet$ (step (II))			
2a+O$_2$→ **3a**	−32	−33	−22
2b+O$_2$→ **3b**	−30	−31	−19
2c+O$_2$→**3c**	−29	−30	−19
ROO$^\bullet$+RH→ROOH+R$^\bullet$ (steps I+III)			
3a+**1**→**4a**+**2a**	11	12	11
3a+**1**→**4a**+**2b**	11	11	11
3a+**1**→**4a**+**2c**	10	11	10
3b+**1**→**4b**+**2a**	9	10	10
3c+**1**→**4c**+**2a**	11	11	10
HOO$^\bullet$+**1**→H$_2$O$_2$+**2a**	11	11	10

activities of the α-oxy hydrogen atoms in **1**. Likewise, we used the reaction with the CH_2 hydrogen atoms adjacent to the OH group of **1** to test the relative abstraction power of peroxyl radicals **3** and also that of free hydroperoxyl radical. As can be seen in Table 1, all such processes are equally unfavorable; they are all endothermic and endergonic by approximately 10 kcal mol^{-1}, due to the relatively high stability of the peroxyl radicals. However, since the following step is barrierless and only limited by diffusion of oxygen, the reaction will proceed despite the unfavorable energetics, only limited by the barrier for hydrogen abstraction. The activation free energies for formation of **2a** and **2b** are 20 kcal mol^{-1}, and slightly higher, 22 kcal mol^{-1}, for the formation of **2c** (see Scheme 3). We found only minor differences between the energies of the three α-oxy radicals (Table 1).[14] Radical **2c** is the most stable one, but only by 1 kcal mol^{-1} relative to **2a** and **2b**, and the barriers to formation of each are similar. Hence, with these small differences, all α-oxy positions of ethoxylated alcohols would be expected to have a similar reactivity in radical-chain processes.

To summarize, one cycle of the chain process is exergonic by approximately 10 kcal mol^{-1} and has a barrier of approximately 20 kcal mol^{-1}. Since this barrier is relatively high, we also explored alternative reaction pathways for the peroxyl radicals **3**. Competing with the second propagation step is an intramolecular rearrangement in which the peroxyl group of radicals **3a**, **3b**, and **3c** abstracts a hydrogen atom within the molecule instead of from an adjacent molecule. The intermediate radicals could presumably react with a second oxygen molecule,[15] but in the current study, we have limited ourselves to products derived from the addition of one molecule of O_2 only. There are different possibilities for the intramolecular hydrogen abstraction for the three radicals, shown in detail in Scheme 4. The fragmentation of **3a** may produce the al-

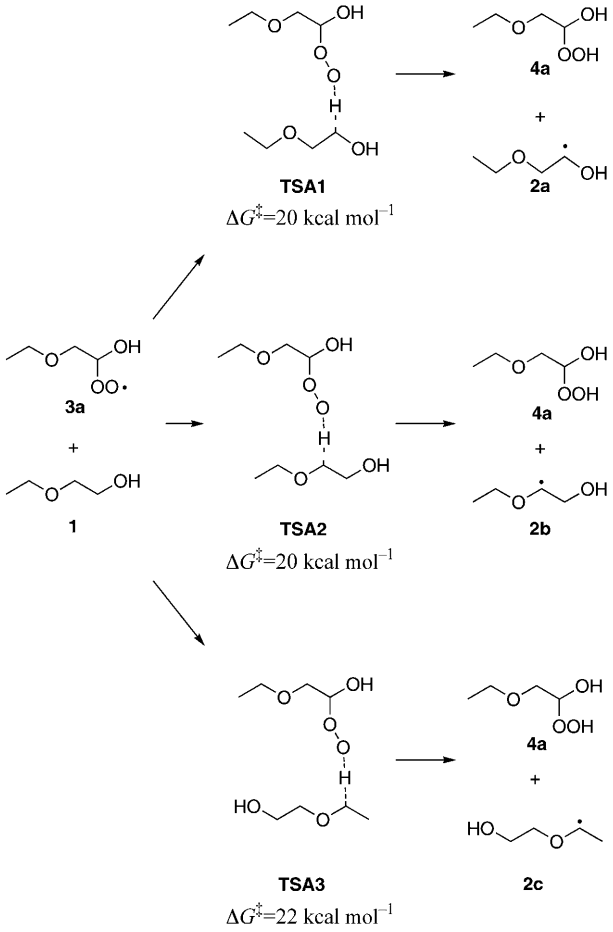

Scheme 3. Activation free energies for the intermolecular hydrogen abstractions by using peroxyl radical **3a** as a model radical.

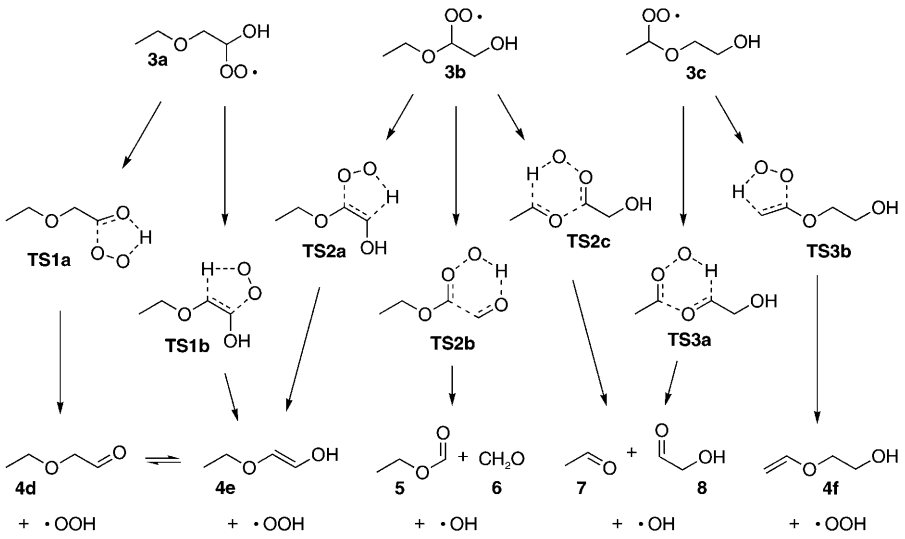

Scheme 4. Intramolecular hydrogen abstraction pathways from peroxyl radicals **3**.

dehyde **4d** or the enol **4e** that in turn rearranges to the aldehyde **4d** by tautomerization. From **3b**, the possible products are the enol **4e**, the formate **5**+formaldehyde **6**, or the aldehydes **7** and **8**. The latter can also result from fragmentation of **3c**, but here an alternative is to form the vinyl ether **4f**. In all cases, the fragmentation also produces either a hydroxyl or hydroperoxyl radical that may propagate the radical-chain reaction.

There are two plausible fragmentation pathways for **3a**, one involving the hydrogen atom of the OH group (**TS1a**) and another involving a hydrogen atom from the adjacent CH_2 group (**TS1b**). The calculated free energies for these processes are depicted in Figure 1. For comparison, the bimolecular propagation step converting **3a** to **4a** has a barrier of 20 kcal mol^{-1}. As can be seen, the intramolecular hydrogen atom abstraction from carbon has a barrier that is substantially higher, 29 kcal mol^{-1}. On the other hand, the intramolecular H-atom abstraction from oxygen has a barrier of only 9 kcal mol^{-1} and is clearly the preferred path for **3a**.[16] Comparison of bimolecular and unimolecular pathways are of doubtful validity, since the standard state is different from the actual concentrations in solution, but the systematic error should not be larger than a few kcal mol^{-1}. Another complicating factor is that the intramolecular rearrangement will be impeded by hydrogen-bond formation, but again, the expected correction is much smaller than the difference in barriers. We note that the product of this process, **4d**, corresponds to the major product in our experimental studies (Scheme 1e).[4]

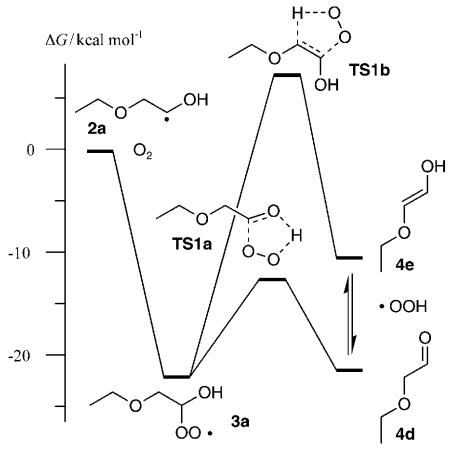

Figure 1. Free-energy profile for unimolecular reactions of **3a**.

Fragmentation of **3b**, shown in Figure 2, is substantially more complex than that of **3a**. There are three possible hydrogen atoms to be abstracted: from the adjacent CH_2 group (**TS2a**), from the OH group (**TS2b**), and from the CH_2 group across the ether oxygen (**TS2c**). Only one of the initially postulated paths corresponds to a concerted process, via **TS2a** to enol **4e**. As before, the formation of **4e** is endergonic, but a tautomeric equilibrium leads to aldehyde **4d** in an overall exergonic process. However, the barrier is fairly high, 25 kcal mol^{-1}. The other two investigated intramolecular hydrogen abstractions lead to shallow intermediates through barriers of 19 kcal mol^{-1}, but both intermediates would mostly be expected to revert to **3b**. Further fragmentation along these paths requires passing **TS2d** or **TS2e**, both with free energies around 25 kcal mol^{-1} higher than that of **3b**. However, the fragmentation into three molecules (two carbonyl compounds and a hydroxyl radical) makes the processes strongly exergonic, and thus completely irreversible. Some of the products formed on long-time exposure to air (Scheme 1) correspond to the model compounds **4d** and **5**–**8**. Thus, these unimolecular fragmentation pathways are probably competitive with the bimolecular propagation steps under experimental conditions, especially when considering that the chemical activity of oxygen is lower than the standard state assumed in the calculations.

Finally, for **3c**, the possible hydrogen abstractions, shown in Figure 3, are from the CH_2 group on the opposite side of the ether oxygen atom (**TS3a**), and from the adjacent alkyl chain, here modeled by a methyl group (**TS3b**). The former is again a simple hydrogen abstraction with a moderate barrier (21 kcal mol^{-1}), followed by a fragmentation step (**TS3c**), which yields aldehyde products **7** and **8** with an overall barrier of 25 kcal mol^{-1} from **3c**. Fragmentation via **TS3b** is concerted, leading to vinyl ether **4f** and hydroperoxyl radical in a process that is endergonic by 8 kcal mol^{-1} and has a barrier of 23 kcal mol^{-1}. Thus, vinyl ethers similar to **4f** are not stable under the reaction conditions, but would revert to **3c** or through other similar paths. Consis-

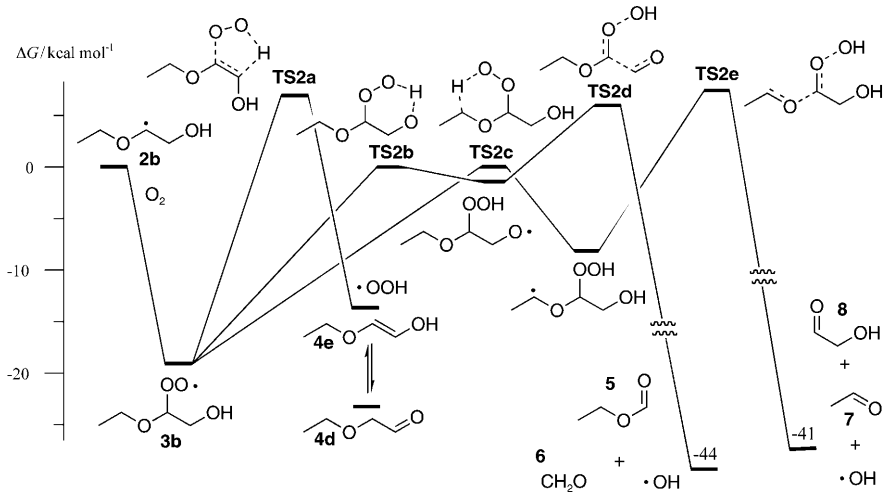

Figure 2. Free-energy profile for unimolecular reactions of **3b**.

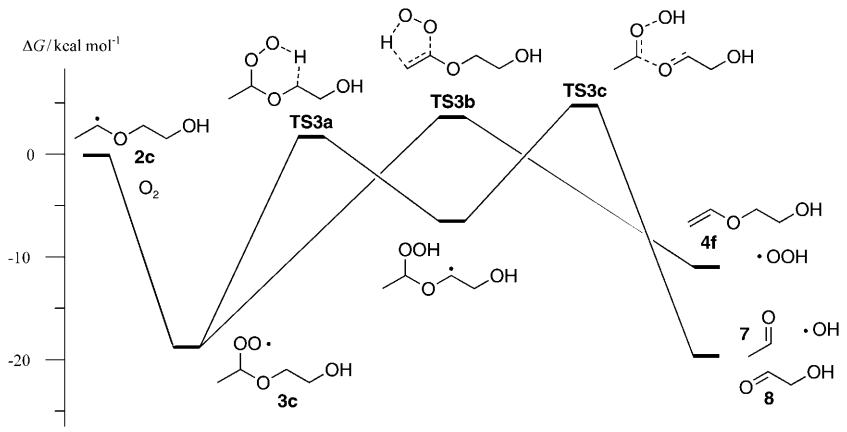

Figure 3. Free-energy profile for unimolecular reactions of **3c**.

tent with this, no vinyl ethers were identified in the experimental studies. An oxidation process via the radicals **2c** and **3c** would be the expected pathway when the polyethoxy moieties of surfactants are fragmented by air oxidation.

Some intramolecular abstraction channels produce hydrogen peroxyl radicals, which may abstract a hydrogen atom from the surfactant molecule (**1**) and form hydrogen peroxide. The reaction energy for the reaction of compound **1** with HOO$^{\bullet}$ is similar to those for reaction between compound **1** and the peroxyl radicals **3a**–**c** (Table 1). Hydrogen peroxide may also be formed by means of acid-catalyzed degradation of hydroperoxide **4a**, which is the least stable of the different hydroperoxides formed by the radical-chain reaction. The decomposition reaction is exergonic by 2 kcal mol^{-1}. Hydrogen peroxide has not been identified in our experiments so far, but the current results show that it is likely to be present, as has already been shown in earlier studies of a related process, the combustion of diethyl ether.[17]

The possibility for hydroperoxide **4a** to fragment into aldehyde **4d** and H_2O_2 shows that the normal radical-chain reaction gives a parallel explanation as to why aldehydes are found in experiments. Hence aldehydes may form both by an intra- and intermolecular reaction path. Most likely both reaction paths coexist.[17]

Conclusion

In this study ethyleneglycol mono ethylether (**1**) was used as a model compound in theoretical calculations to investigate product formation in the autoxidation of pentaethylene glycol mono *n*-dodecyl ether $C_{12}E_5$ that we have previously investigated experimentally. We have studied two different reaction channels: the normal intermolecular radical-chain mechanism, which yields hydroperoxides, and intramolecular hydrogen-abstraction pathways, which give rise to aldehydes, formates, and α-hydroxy (and possibly α-alkoxy) aldehydes. We found the radical-chain reaction to include an endergonic step, which points at slow development, in accordance with the experimental results.

Our computational calculations of the model system show that the various reaction energies in the radical-chain mechanism are similar and do not explain why one hydroperoxide is significantly favored over another. On the other hand, one of the hydroperoxides is more prone to decompose and form the aldehyde seen in experiments. Hence this is a possible explanation of aldehyde formation. The inclusion of an intramolecular hydrogen-abstraction pathway gives an additional explanation of the product distribution. Here, the reaction and the activation energies show a possibility to form an aldehyde corresponding to the main aldehyde seen in experiments. For peroxyl radicals formed at the alkyl end (here modeled by **3c**), hydrogen abstraction from the alkyl chain would be disfavored, and thus the likelihood of propagation to form the hydroperoxide increased. This agrees with the experimental results, in which the dominating hydroperoxide found corresponds to **4c**.

Acknowledgement

This research is supported by the Swedish Research Council (VR).

[1] M. Donbrow in *Nonionic Surfactants, Vol. 23: Physical Chemistry* (Ed. M. J. Schick), New York, Surfactant Science Series, **1987**, pp. 1011–1067.
[2] E. T. Denisov, I. B. Afanas′ev, *Oxidation and Antioxidants in Organic Chemistry and Biology*, Taylor&Francis, Boca Raton, **2005**.
[3] A.-T. Karlberg, A. Bodin, M. Matura, *Contact Dermatitis* **2003**, *49*, 241–247.
[4] M. Bergh, L. P. Shao, G. Hagelthorn, E. Gäfvert, J. L. G. Nilsson, A.-T. Karlberg, *J. Pharm. Sci.* **1998**, *87*, 276–282.
[5] A. Bodin, T. Fischer, M. Bergh, J. L. G. Nilsson, A.-T. Karlberg, *Contact Dermatitis* **2000**, *43*, 82–89.
[6] M. Bergh, L. P. Shao, G. Hageltorn, E. Gäfvert, J. L. G. Nilsson, A.-T. Karlberg, *J. Pharm. Sci.* **1999**, *88*, 483–488.
[7] A. Bodin, L. P. Shao, J. L. G. Nilsson, A.-T. Karlberg, *Contact Dermatitis* **2001**, *44*, 207–212.
[8] A. Bodin, M. Linnerborg, J. L. G. Nilsson, A.-T. Karlberg, *Chem. Res. Toxicol.* **2003**, *16*, 575–582.
[9] M. Bergh, A.-T. Karlberg, *Contact Dermatitis* **1999**, *40*, 139–145.
[10] A. Bodin, M. Linnerborg, J. L. G. Nilsson, A.-T. Karlberg, *J. Surfactants Deterg.* **2002**, *5*, 107–110.
[11] C. Bäcktorp, L. Hagvall, A. Börje, A.-T. Karlberg, P.-O. Norrby, G. Nyman, *J. Chem. Theory Comput.* **2008**, *4*, 101–106.
[12] a) C. Lee, W. Yang, R. G. Parr, *Phys. Rev. B* **1988**, *37*, 785–789; b) A. D. Becke, *J. Chem. Phys.* **1993**, *98*, 1372–1377; c) A. D. Becke, *J. Chem. Phys.* **1993**, *98*, 5648–5652 d) P. J. Stephens, F. J. Devlin, C. F. Chabalowski, M. J. Frisch, *J. Phys. Chem.* **1994**, *98*, 11623–11627.
[13] Gaussian 03 (Revision D.02), M. J. Frisch, G. W. Trucks, H. B. Schlegel, G. E. Scuseria, M. A. Robb, J. R. Cheeseman, J. A. Montgomery, Jr., T. Vreven, K. N. Kudin, J. C. Burant, J. M. Millam, S. S. Iyengar, J. Tomasi, V. Barone, B. Mennucci, M. Cossi, G. Scalmani, N.

Rega, G. A. Petersson, H. Nakatsuji, M. Hada, M. Ehara, K. Toyota, R. Fukuda, J. Hasegawa, M. Ishida, T. Nakajima, Y. Honda, O. Kitao, H. Nakai, M. Klene, X. Li, J. E. Knox, H. P. Hratchian, J. B. Cross, V. Bakken, C. Adamo, J. Jaramillo, R. Gomperts, R. E. Stratmann, O. Yazyev, A. J. Austin, R. Cammi, C. Pomelli, J. W. Ochterski, P. Y. Ayala, K. Morokuma, G. A. Voth, P. Salvador, J. J. Dannenberg, V. G. Zakrzewski, S. Dapprich, A. D. Daniels, M. C. Strain, O. Farkas, D. K. Malick, A. D. Rabuck, K. Raghavachari, J. B. Foresman, J. V. Ortiz, Q. Cui, A. G. Baboul, S. Clifford, J. Cioslowski, B. B. Stefanov, G. Liu, A. Liashenko, P. Piskorz, I. Komaromi, R. L. Martin, D. J. Fox, T. Keith, M. A. Al-Laham, C. Y. Peng, A. Nanayakkara, M. Challacombe, P. M. W. Gill, B. Johnson, W. Chen, M. W. Wong, C. Gonzalez, and J. A. Pople, Gaussian, Inc., Wallingford CT, **2004**.

[14] T. G. Denisova, N. S. Emel′yanova, *Kinet. Catal.* **2003**, *44*, 441–449.

[15] A. Andersen, E. A. Carter, *J. Phys. Chem. A* **2003**, 107, 9463–9478.

[16] J. C. Rienstra-Kiracofe, W. D. Allen, H. F. Schaefer III, *J. Phys. Chem. A* **2000**, *104*, 9823–9840.

[17] K. C. Salooja, *Combust. Flame* **1965**, *9*, 33–41.

Received: March 25, 2008
Published online: September 11, 2008

